

An Anisotropic Diffusion Adaptive Filter for Image Denoising and Restoration Applied on Satellite Remote Sensing Images

A Case Study

Messaouda Gatcha
AAID Laboratory
Faculty of Exact Sciences and Computers
Ziane Achour University
Djelfa, Algeria
messaoudamath2017@gmail.com

Farid Messelmi
DMM Laboratory
Faculty of Exact Sciences and Computers
Ziane Achour University
Djelfa, Algeria
foudimath@yahoo.fr

Slami Saadi
AAID Laboratory
Faculty of Exact Sciences and Computers
Ziane Achour University
Djelfa, Algeria
saadisdz@gmail.com

Received: 22 September 2022 | Revised: 1 October 2022 | Accepted: 2 October 2022

Abstract-This paper proposes an operating approach based on the anisotropic diffusion method to restore and denoise Satellite Remote Sensing Images (SRSIs). The contents of the approach are the motion by mean curvature to detect the noise direction for each degraded pixel and preserve the original edges of the image, and the gradient in the Gaussian kernel which restores the degraded pixel locally, assuring the estimation of its original value and saving the contrast of the image. The algorithm, concluded by our proposed system, treats noised SRSIs regardless of noise type, so better restoration is achieved. Experiments of the proposed system and of other approaches were conducted in MATLAB in order to demonstrate the efficiency of the proposed approach and its performance was confirmed through evaluation with PSNR and SSIM.

Keywords-image restoration; anisotropic diffusion; regularization; satellite remote sensing images

I. INTRODUCTION

Satellite Remote Sensing Images (SRSIs) are known for their fussy response or tendency to be corrupted due to multiple aspects of noise that might occur, such as time, feedbacks, accuracy, lighting, landforms, surface reflections, and reflection angles. Mathematically, image denoising is an ill-posed problem due to the fact that the added noise has divergent characteristics. Partial Differential Equations (PDE) in the anisotropic diffusion method provide a safe executive solution for image restoration, as a consequence of the multidirectional gradient through the noised (corrupted) pixel

neighborhoods, and assist an easy transpass from a system to another when we change the noise type.

The earlier works in the image denoising field, start with the Marr-Hildreth edge detector [1] by finding the zero-crossing of the second derivative D^2 of intensity. Author in [2] considers the image structure using the divergence of the image, focusing on blurred ones. Perona-Malik equation [3] has been applied many times. In [4], motion by mean curvature appears in the degenerate diffusion term, which diffuses the image in the orthogonal direction to its gradient and does not diffuse at all in the direction of the gradient. More recently, authors in [5], proposed an improved Empirical Mode Decomposition and Adaptive Center-Weighted Average (EMD-ACWA) denoising scheme by estimating the noise energies of all intrinsic mode functions, using an energy model, called noise-only model. It turns out that the empirical mode decomposition acts on fractional Gaussian noise as a dyadic filter bank. Authors in [6] worked on speckle noise elimination. The denoising research was applied to color images in [7].

There are many studies regarding SRSIs [8] using different techniques, such as as curvelet transform [9], wavelet packet transform [10], multifractal analysis[11], undecimated discrete wavelet transform [12], etc.

II. RECENT WORKS ABOUT SATELLITE REMOTE SENSING IMAGE DENOISING

Authors in [13] extended the existing learning-based methods in several aspects. Their work combines a realistic

Corresponding author: Messaouda Gatcha

physical noise model of the camera with real noise samples from dark frames to generate realistic training data. They formulated a physical noise model for a Charge Coupled Device (CCD) sensor and presented a novel application of learning-based lowlight image denoising suitable for lunar surface images. They combined a physical noise model with real noise samples and scene selection based on three dimension (3D) ray tracing to generate training data and by conditioning the model on the camera's environmental metadata at the time of image capture.

Authors in [14] resort to the Plug-and-Play (PnP) framework to address the Hyperspectral Image (HSI) denoising task by proposing a PnPHSI (Plug-and-Play- Hyperspectral Images) denoising model with low-rank representation and a prior CNN (Convolutional Neural Network) denoiser. In the proposed PnP framework, the eigen-images are denoised by a DRUNet (Dilated-Residual U-NET) submodel. In [15], the enhanced Adaptive Generalized Gaussian Distribution (AGGD) and the improved AGGD threshold function enhanced the qualitative and quantitative results of TNN and optimization-based noise removal. The improved AGGD consists of two main parts. In the interval $[-t, t]$, the function is adaptive GGD (Generalized Gaussian Distribution), and behind the interval, it is a non-linear function.

III. THE PROPOSED METHOD FOR SATELLITE REMOTE SENSING IMAGES DENOISING

In this paper, we propose an Anisotropic Diffusion approach on the basis of PDE, containing motion by mean curvature, convolution product, Gaussian kernel, and time of processing term:

$$\begin{cases} I_t = c(t) \cdot |\nabla G_\sigma * I| \cdot |\nabla I| \cdot \text{div} \left(\frac{\nabla I}{|\nabla I|} \right) \\ I(0, x, y) = I_0(x, y) \end{cases} \quad (1)$$

where I_t is the enhanced image from the noised image I and $c(t) = 1 + \frac{1}{\sqrt{4+t^2}}$ is the diffusion problem coefficient term

that helps to enhance the image contrast and keeps it from turning darker during the execution process. The motion by the mean curvature term is the degenerated diffusion term

$|\nabla I| \cdot \text{div} \left(\frac{\nabla I}{|\nabla I|} \right)$ which precises the noised pixel and noise

direction in its multidirectional neighboring, and $|\nabla G_\sigma * I|$ is the Gaussian kernel mask with σ standard deviation. For noised pixel restoration we used a $\sigma \times \sigma$ mask to redefine the value of the noised pixel from its neighboring pixels.

The numerical solution of the PDE in the earlier system, is found by the Finite Differences (FD) method [16], Simpsons improved method [16], and the convolution product [17, 18], where the image pixel is the step for the mesh required in the numerical treatment of the image, that means we will work locally for each pixel in the digital image. For the image

clarification sought during the image acquisition process, the time step is calculated as:

$$\tau = \frac{T}{N} \quad (2)$$

where T is the time range, N' the number of iterations, and $k=1..T$ the time index.

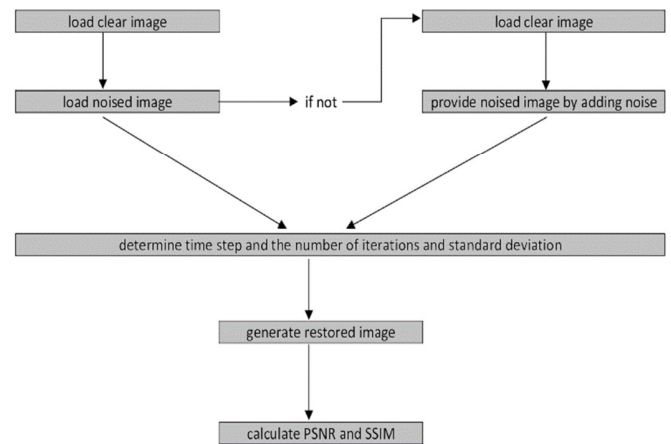


Fig. 1. The image regularization process.

IV. PROBLEM STABILITY

In this section, the following theorem is used to prove the stability of the proposed method [19].

Theorem: Let $L.U = f$ be the problem and $L.U^{(h)} = f^{(h)}$ its perturbed version. The Euler explicit schema of the problem $L.U = f$ is stable if $\exists \delta > 0; \exists h_0 > 0 \forall h < h_0, \forall \delta f^{(h)} \in F_h$ such that $L.U^{(h)} = f^{(h)} + \delta f^{(h)}$ accepts a unique solution $Z^{(h)} \in U_h$. Furthermore: $\|Z^{(h)} - U^{(h)}\|_{U_h} \leq \alpha \|f^{(h)}\|_{F_h}$, where α is a constant, $Z^{(h)}$ the approximated solution, U_h the approximated solution space, $f^{(h)}$ the approximated function, and F_h the approximated function space.

We apply the previous theorem on our problem, when the subset Ω is associated with the norm sup.

In $I_t = \frac{\partial I}{\partial t}$ the operator $\frac{\partial}{\partial t}$ is linear, so we prove that $\|I^{(h)}\|_{\Omega_h} \leq \alpha \|f^{(h)}\|_{\Omega_h}$, where $I_t = \frac{I(t+1,x,y) - I(t,x,y)}{\tau}$, I is the image, and $I_t = f(k, i, j)$, so we have $\frac{I(k+1,i,j) - I(k,i,j)}{\tau} = f(k, i, j)$. Then we have:

$$I(k+1, i, j) = I(k, i, j) + \tau \cdot f(k, i, j)$$

$$|I_{ij}^{k+1}| = |I_{ij}^k + \tau \cdot f_{ij}^k|$$

$$\max_{i,j} |I_{ij}^k| \leq \max_{i,j} |I_{ij}^{k-1}| + \tau \cdot \max_{i,j} |f_{ij}^k|$$

$$\max_{i,j} |I_{ij}^1| \leq \max_{i,j} |I_{ij}^0| + \tau \cdot \max_{i,j} |f_{ij}^k|$$

By adding side by side, we get:

$$\max_{i,j} |I_{ij}^k| \leq \max_{i,j} |I_{ij}^0| + n.\tau. \max_{i,j} |f_{ij}^k|$$

$$\|I^{(h)}\|_{\Omega_h} \leq \alpha \|f^{(h)}\|_{\Omega_h}$$

where the schema is stable for $\alpha = 1+T$.

V. RESULTS AND DISCUSSION

In order to estimate the efficiency of the proposed image restoration model, we applied it on different types of noise (salt and pepper, Gaussian, speckle). We carried out the algorithm simulations using a Windows 32 bit PC powered by an Intel 2.6GHz processor with 2GB RAM. The experiments were performed in MATLAB R2017 [20, 21] due to its image processing toolbox, with time intervals took between $\tau=01s$ and $\tau=60s$ according to the image size and the number for iterations, noting that :

- PSNR: Peak Signal to Noise Ratio. It gives a noise free $m \times n$ monochrome for image I and its noisy approximation.
- SSIM: Structure Similarity Index metric. It is a method for predicting the perceived quality of measuring the similarity between two images, usually an original and a restored image.

The Euler Explicit schema extracted from the discretization of the system (1) concludes the algorithm programmed in MATLAB and gives the process to the noised image restoration. The manipulation gets into the following steps:

- Step 1: Program the convolution product based on the Gaussian kernel as a $\sigma \times \sigma$ mask with σ standard deviation and scale parameter.
- Step 2: Verify the image dimension that should be $\dim(I)=2$. Then convert the image grayscale with single values for pixels.
- Step 3: Filter the image by motion by mean curvature to detect degraded pixels.
- Step 4: Determine time step τ , number of iterations K , and standard deviation σ .
- Step 5: Start a loop from $k=1$ to $k=K$ restoring the degraded pixels and enhancing the image, calculating PSNR and SSIM to measure the improvement from the achieved results.

Tables II-IV demonstrate the manipulation results for different types of noise applied on the images (Figures 1-5) in Table I. The iteration number of the denoising process is between 10 and 20 for remarkable enhancement with high PSNR, whilst Table V describes a comparison with the results obtained by the works mentioned above (see Section II) and the obtained results by the proposed Anisotropic Diffusion method where there is a round-trip in PSNR and the clarity of images.

TABLE I. IMAGE DESCRIPTION

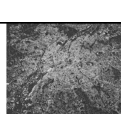
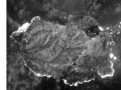

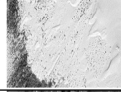

| | | Image size | Image name |
|----------|--|------------|--|
| Figure 1 |  | 1.28 mega | Map of Brussels view satellite-Belgium |
| Figure 2 |  | 520 ko | Band8 crop chip |
| Figure 3 |  | 812 ko | Shannon Airplane Irlande |
| Figure 4 |  | 925 ko | Algerian Sahara |
| Figure 5 |  | 1.02 mega | IRLANDE |

TABLE II. REDUCED SALT AND PEPPER NOISE FOR $D=0.1, K=10$

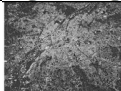
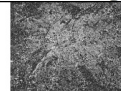
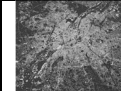
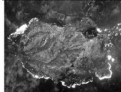
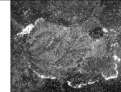
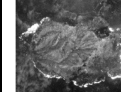


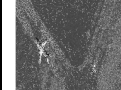
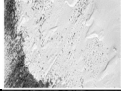

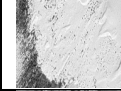



| Original image | Noised image | Restored image | PSNR | SSIM |
|---|---|---|---------|--------|
|  |  |  | 29.3953 | 0.5774 |
|  |  |  | 27.4245 | 0.8199 |
|  |  |  | 30.2833 | 0.7961 |
|  |  |  | 27.6886 | 0.8725 |
|  |  |  | 26.3484 | 0.8521 |

TABLE III. REDUCED GAUSSIAN NOISE $\sigma = 0.1, K=10$

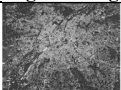
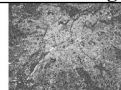
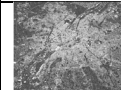

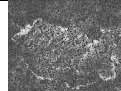
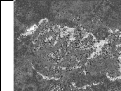





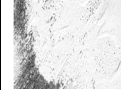



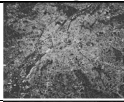
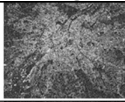
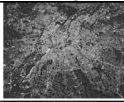
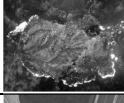
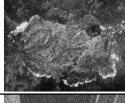
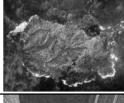



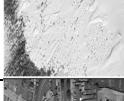





| Original image | Noised image | Restored image | PSNR | SSIM |
|---|---|---|---------|--------|
|  |  |  | 31.7707 | 0.5347 |
|  |  |  | 28.9869 | 0.6346 |
|  |  |  | 28.7726 | 0.5922 |
|  |  |  | 27.8323 | 0.7509 |
|  |  |  | 29.4133 | 0.6985 |

TABLE IV. REDUCED SPECKLE NOISE $\sigma = 0.1, K = 20$


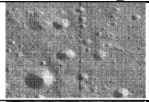
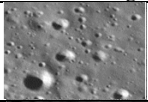


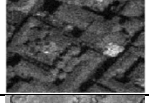






| Original image | Noised image | Restored image | PSNR | SSIM |
|---|---|---|---------|--------|
|  |  |  | 30.2091 | 0.5137 |
|  |  |  | 24.1765 | 0.6187 |
|  |  |  | 25.2453 | 0.5092 |
|  |  |  | 27.8884 | 0.4084 |
|  |  |  | 25.4414 | 0.6341 |

The algorithm outperforms the other approaches regarding the regularization of the noised image for Gaussian and speckle noise. It also did not turn the image darker due to the gradient, as can be also seen in the comparison part.

VI. CONCLUSION

Image denoising and enhancement in order to improve image quality for more exact information extracting is a trending research topic. Especially the capturing of Satellite Remote Sensing Images has the obstacle of the long distance barrier between objects and sensors, so captured images are more liable for noise like environment effects, light concentration and camera sharpness. The partial differential equation systems give a reliable point of view that helps this development, based on the multidirectional gradient that allows noise detection in several directions independently and locally for better regularization, unlike the total variation method which treats the noised image globally.

TABLE V. COMPARISON RESULTS WITH RECENT WORKS

| | Other works | | | | Proposed | |
|------|---|---|---|-------|---|-------|
| | Original image | Noised image | Restored image | PSNR | Restored image | PSNR |
| [13] |  |  |  | 43.33 |  | 38.58 |
| [14] |  |  |  | 42.14 |  | 40.76 |
| [15] |  |  |  | 34.27 |  | 35.79 |

REFERENCES

[1] D. Marr and E. Hildreth, "Theory of edge detection," *Proceedings of the Royal Society of London, Series B. Biological Sciences*, vol. 207, no. 1167, <https://doi.org/10.1098/rspb.1980.0020>.

[2] J. J. Koenderink, "The structure of images," *Biological Cybernetics*, vol. 50, pp. 363–370, 1984.

[3] P. Perona and J. Malik, "Scale-space and edge detection using anisotropic diffusion," *IEEE Transactions on Pattern Analysis and Machine Intelligence*, vol. 12, no. 7, pp. 629–639, Jul. 1990, <https://doi.org/10.1109/34.56205>.

[4] L. Alvarez, P.-L. Lions, and J.-M. Morel, "Image Selective Smoothing and Edge Detection by Nonlinear Diffusion. II," *SIAM Journal on numerical analysis*, vol. 29, no. 3, pp. 845–866, Jun. 1992, <https://doi.org/10.1137/0729052>.

[5] I. Tellala, N. Amardjia, and A. Kesmia, "A Modified EMD-ACWA Denoising Scheme using a Noise-only Model," *Engineering, Technology & Applied Science Research*, vol. 10, no. 2, pp. 5470–5476, Apr. 2020, <https://doi.org/10.48084/etasr.3406>.

[6] N. Diffellah, R. Hamdini, and T. Bekkouche, "Removal of Multiplicative Gamma Noise from Images via SRAD Model Amelioration," *Engineering, Technology & Applied Science Research*, vol. 11, no. 6, pp. 7917–7921, Dec. 2021, <https://doi.org/10.48084/etasr.4527>.

[7] M. V. Sarode and P. R. Deshmukh, "Image Sequence Denoising with Motion Estimation in Color Image Sequences," *Engineering, Technology & Applied Science Research*, vol. 1, no. 6, pp. 139–143, Dec. 2011, <https://doi.org/10.48084/etasr.54>.

[8] J. Gao, *Digital Analysis of Remotely Sensed Imagery*, 1st ed. McGraw Hill, 2009.

[9] F. Nencini, A. Garzelli, S. Baronti, and L. Alparone, "Remote sensing image fusion using the curvelet transform," *Information Fusion*, vol. 8, no. 2, pp. 143–156, Apr. 2007, <https://doi.org/10.1016/j.inffus.2006.02.001>.

[10] J. Kang and W. Zhang, "Quickbird Remote Sensing Image Denoising Using Wavelet Packet Transform," in *2008 Second International Symposium on Intelligent Information Technology Application*, Shanghai, China, Sep. 2008, vol. 3, pp. 315–318, <https://doi.org/10.1109/IITA.2008.269>.

[11] M.-G. Hu, J.-F. Wang, and Y. Ge, "Super-Resolution Reconstruction of Remote Sensing Images Using Multifractional Analysis," *Sensors (Basel, Switzerland)*, vol. 9, no. 11, pp. 8669–8683, 2009, <https://doi.org/10.3390/s91108669>.

[12] W. Wang and Y. Li, "Bayesian Denoising for Remote Sensing Image Based on Undecimated Discrete Wavelet Transform," in *2009 International Conference on Information Engineering and Computer Science*, Wuhan, China, Sep. 2009, <https://doi.org/10.1109/ICIECS.2009.5365574>.

[13] B. Moseley, V. Bickel, I. G. López-Francos, and L. Rana, "Extreme Low-Light Environment-Driven Image Denoising over Permanently Shadowed Lunar Regions with a Physical Noise Model," in *2021 IEEE/CVF Conference on Computer Vision and Pattern Recognition*

- (CVPR), Nashville, TN, USA, Jun. 2021, pp. 6313–6323, <https://doi.org/10.1109/CVPR46437.2021.00625>.
- [14] H. Sun, M. Liu, K. Zheng, D. Yang, J. Li, and L. Gao, "Hyperspectral Image Denoising via Low-Rank Representation and CNN Denoiser," *IEEE Journal of Selected Topics in Applied Earth Observations and Remote Sensing*, vol. 15, pp. 716–728, 2022, <https://doi.org/10.1109/JSTARS.2021.3138564>.
- [15] N. A. Golilarz, H. Gao, S. Pirasteh, M. Yazdi, J. Zhou, and Y. Fu, "Satellite Multispectral and Hyperspectral Image De-Noising with Enhanced Adaptive Generalized Gaussian Distribution Threshold in the Wavelet Domain," *Remote Sensing*, vol. 13, no. 1, Jan. 2021, Art. No. 101, <https://doi.org/10.3390/rs13010101>.
- [16] V. S. Riabenki and S. K. Godounov, *Theory of Difference Schemes: An Introduction*. Algeria: University Publication Office, 1987.
- [17] A. Boucher, *Image Processing - Spatial Convolution*. Montreal, QC, Canada: University of Montreal, 2016.
- [18] V. Choqueuse, *Convolution Product - Principle and Propieties*. 2016.
- [19] Z. Li, Z. Qiao, and T. Tang, *Numerical Solution of Differential Equations*. Cambridge University Press, 2017.
- [20] J. C. Russ, *The Image Processing Cookbook*, 4th ed. CreateSpace Independent Publishing Platform, 2017.
- [21] "MathWorks - Makers of MATLAB and Simulink - MATLAB & Simulink," *Mathworks*. <https://www.mathworks.com/>.